Supporting Information

Crystal structure and magnetic properties of $EuZrO_3$ solid solutions

Sihui Li, Shinya Konishi, Takuya Kito, Koji Fujita, and Katsuhisa Tanaka

Department of Material Chemistry, Graduate School of Engineering, Kyoto University, Nishikyo-ku, Kyoto 615-8510, Japan

X-ray diffraction profiles

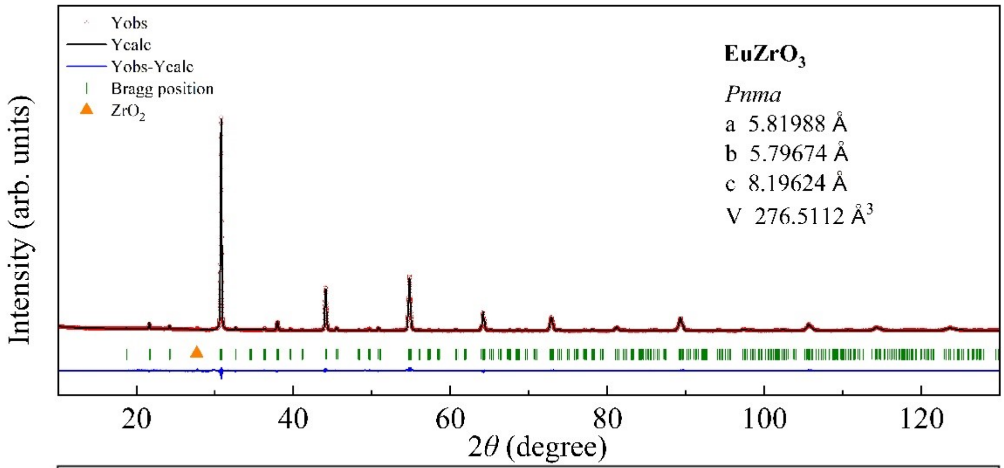

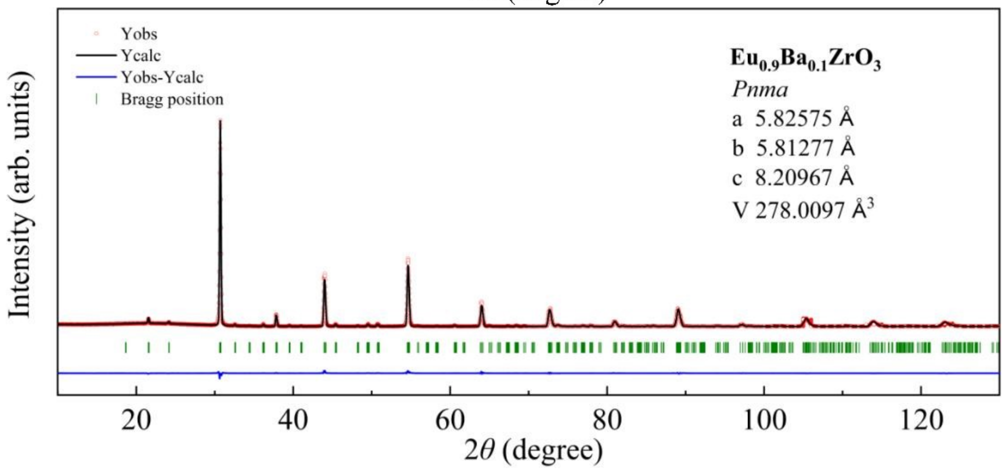

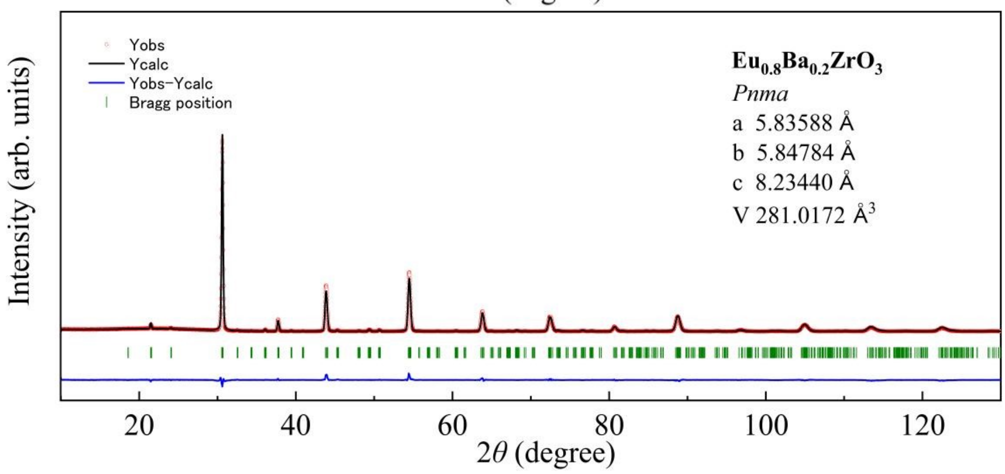

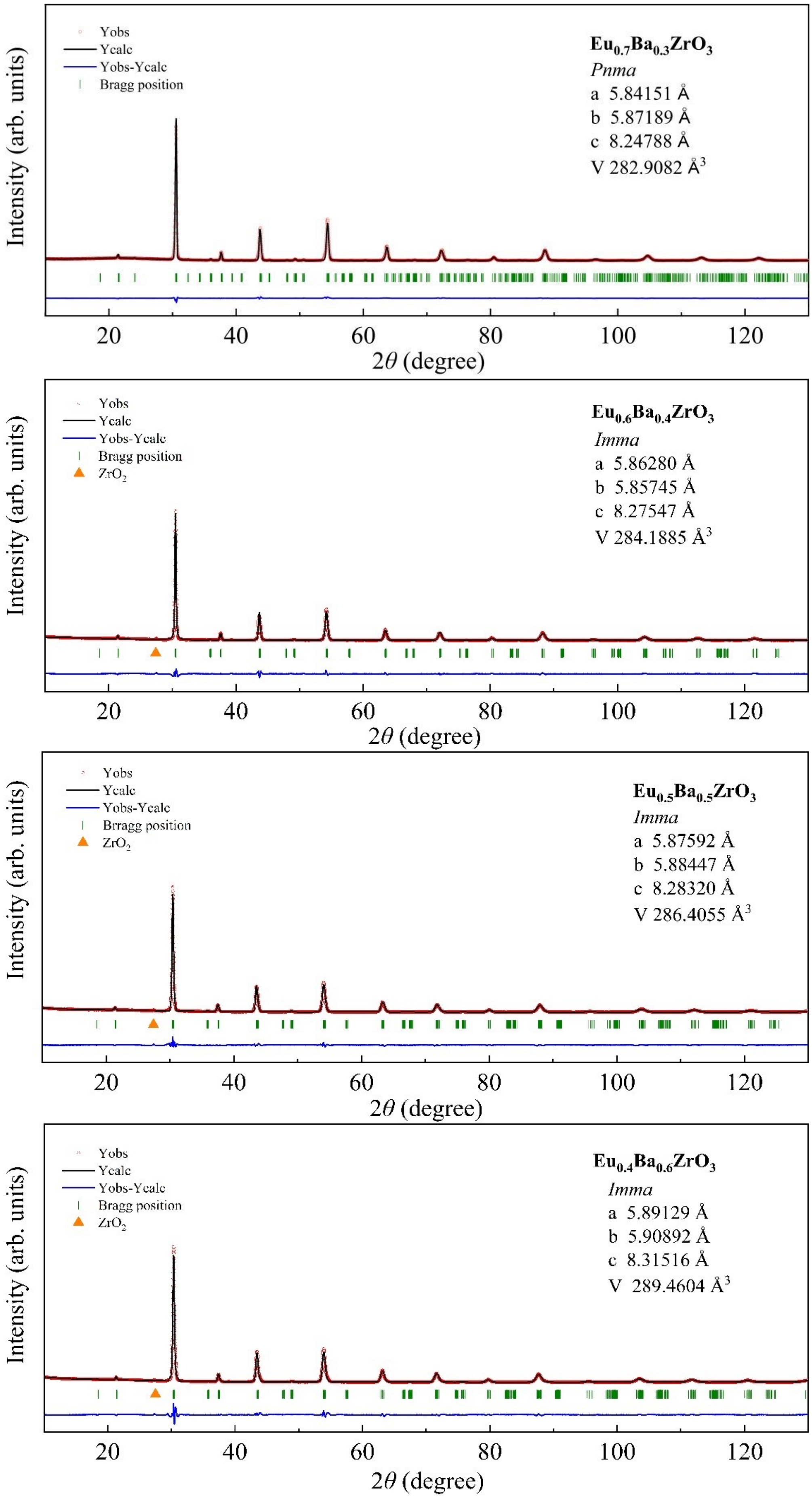

Yobs
Ycalc
Yobs-Ycalc
Bragg position
$Eu_{0.7}Ba_{0.3}ZrO_3$
Pnma
a 5.84151 Å
b 5.87189 Å
c 8.24788 Å
V 282.9082 $Å^3$
Intensity (arb. units)
20 40 60 80 100 120
2θ (degree)
Yobs
Ycalc
Yobs-Ycalc
Bragg position
ZrO_2
$Eu_{0.6}Ba_{0.4}ZrO_3$
Imma
a 5.86280 Å
b 5.85745 Å
c 8.27547 Å
V 284.1885 $Å^3$
Intensity (arb. units)
20 40 60 80 100 120
2θ (degree)
Yobs
Ycalc
Yobs-Ycalc
Brragg position
ZrO_2
$Eu_{0.5}Ba_{0.5}ZrO_3$
Imma
a 5.87592 Å
b 5.88447 Å
c 8.28320 Å
V 286.4055 $Å^3$
Intensity (arb. units)
20 40 60 80 100 120
2θ (degree)
Yobs
Ycalc
Yobs-Ycalc
Bragg position
ZrO_2
$Eu_{0.4}Ba_{0.6}ZrO_3$
Imma
a 5.89129 Å
b 5.90892 Å
c 8.31516 Å
V 289.4604 $Å^3$
Intensity (arb. units)
20 40 60 80 100 120
2θ (degree)

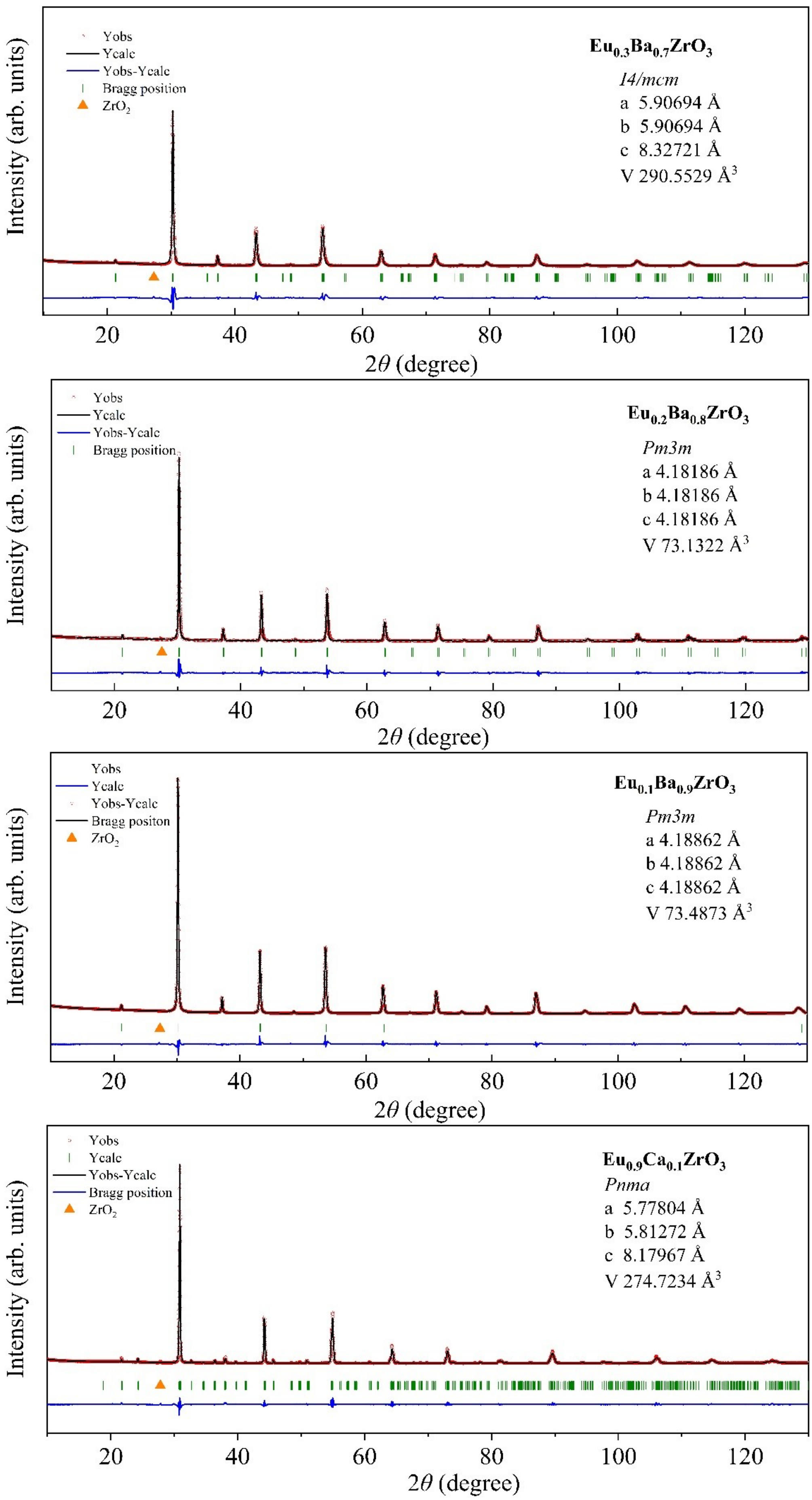
Yobs
Ycalc
Yobs-Ycalc
Bragg position
ZrO$_2$
Eu$_{0.3}$Ba$_{0.7}$ZrO$_3$
I4/mcm
a 5.90694 Å
b 5.90694 Å
c 8.32721 Å
V 290.5529 Å^3
Intensity (arb. units)
2θ (degree)
Yobs
Ycalc
Yobs-Ycalc
Bragg position
Eu$_{0.2}$Ba$_{0.8}$ZrO$_3$
Pm3m
a 4.18186 Å
b 4.18186 Å
c 4.18186 Å
V 73.1322 Å^3
Intensity (arb. units)
2θ (degree)
Yobs
Ycalc
Yobs-Ycalc
Bragg positon
ZrO$_2$
Eu$_{0.1}$Ba$_{0.9}$ZrO$_3$
Pm3m
a 4.18862 Å
b 4.18862 Å
c 4.18862 Å
V 73.4873 Å^3
Intensity (arb. units)
2θ (degree)
Yobs
Ycalc
Yobs-Ycalc
Bragg position
ZrO$_2$
Eu$_{0.9}$Ca$_{0.1}$ZrO$_3$
Pnma
a 5.77804 Å
b 5.81272 Å
c 8.17967 Å
V 274.7234 Å^3
Intensity (arb. units)
2θ (degree)

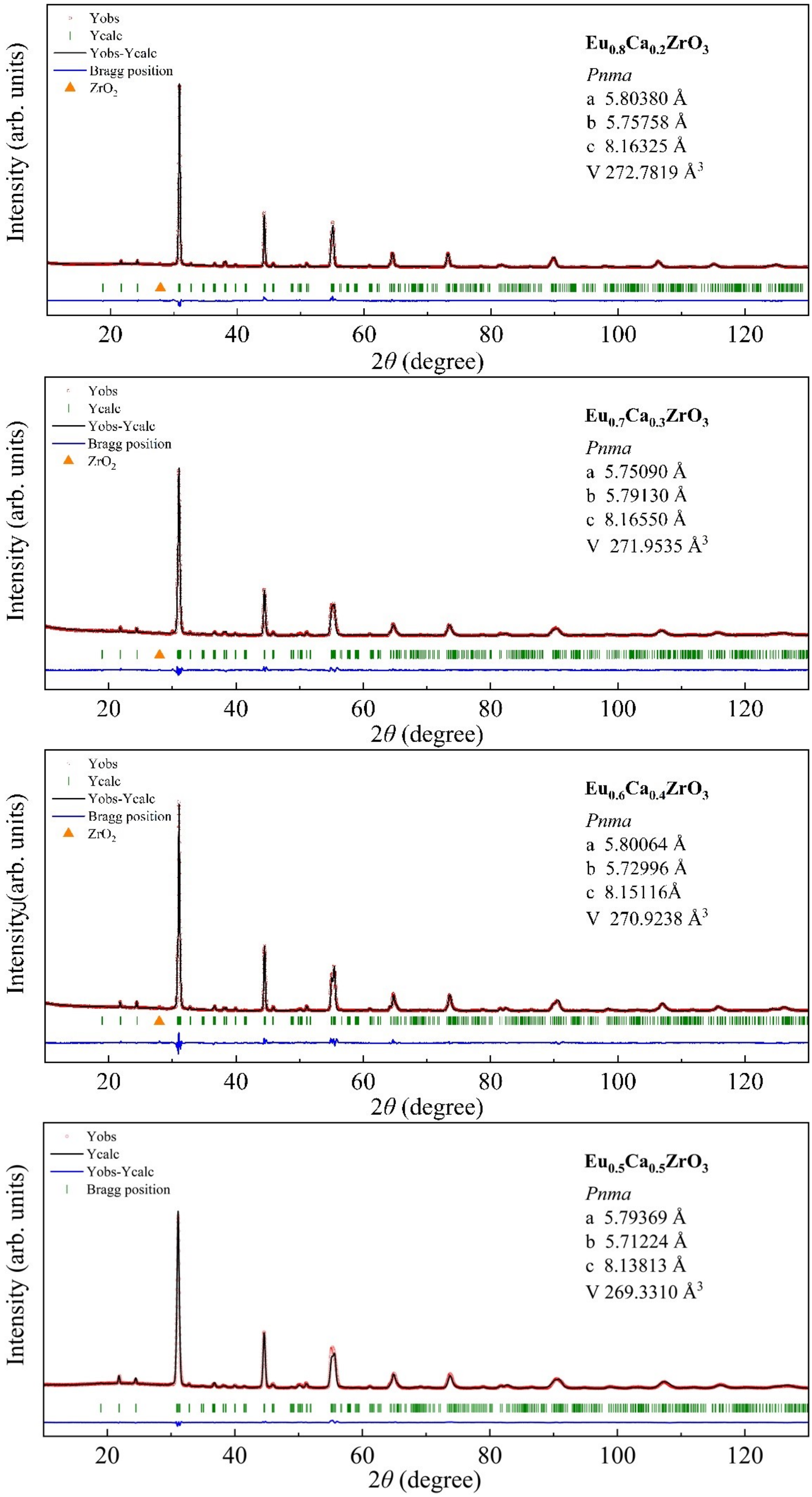
Yobs
Ycalc
Yobs-Ycalc
Bragg position
ZrO2
Eu0.8Ca0.2ZrO3
Pnma
a 5.80380 Å
b 5.75758 Å
c 8.16325 Å
V 272.7819 Å3
Intensity (arb. units)
2θ (degree)
Eu0.7Ca0.3ZrO3
Pnma
a 5.75090 Å
b 5.79130 Å
c 8.16550 Å
V 271.9535 Å3
Eu0.6Ca0.4ZrO3
Pnma
a 5.80064 Å
b 5.72996 Å
c 8.15116Å
V 270.9238 Å3
Eu0.5Ca0.5ZrO3
Pnma
a 5.79369 Å
b 5.71224 Å
c 8.13813 Å
V 269.3310 Å3
20
40
60
80
100
120

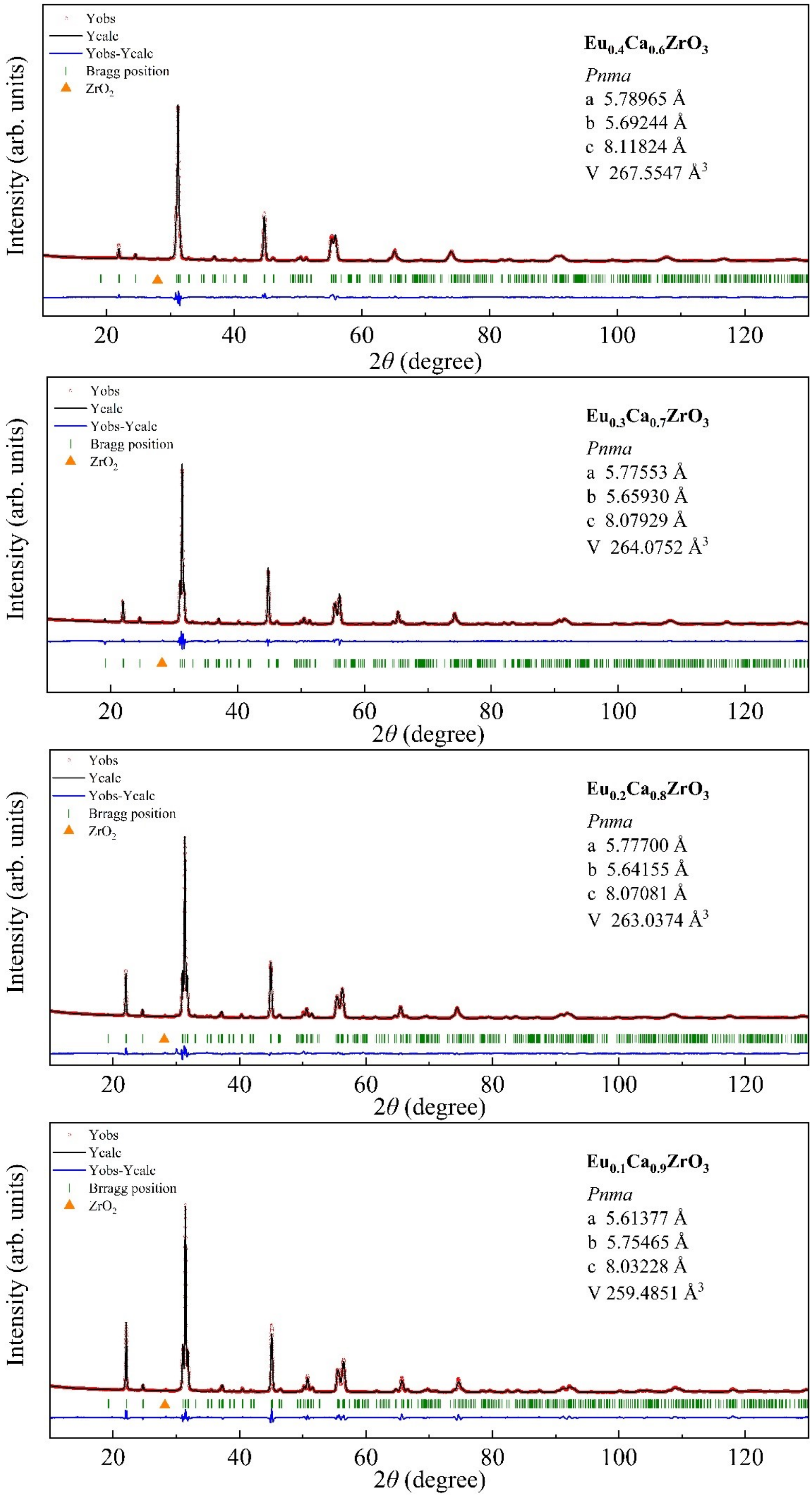
Yobs
Ycalc
Yobs-Ycalc
Bragg position
ZrO2
Eu0.4Ca0.6ZrO3
Pnma
a 5.78965 Å
b 5.69244 Å
c 8.11824 Å
V 267.5547 Å3
Intensity (arb. units)
2θ (degree)
Yobs
Ycalc
Yobs-Ycalc
Bragg position
ZrO2
Eu0.3Ca0.7ZrO3
Pnma
a 5.77553 Å
b 5.65930 Å
c 8.07929 Å
V 264.0752 Å3
Intensity (arb. units)
2θ (degree)
Yobs
Ycalc
Yobs-Ycalc
Brragg position
ZrO2
Eu0.2Ca0.8ZrO3
Pnma
a 5.77700 Å
b 5.64155 Å
c 8.07081 Å
V 263.0374 Å3
Intensity (arb. units)
2θ (degree)
Yobs
Ycalc
Yobs-Ycalc
Brragg position
ZrO2
Eu0.1Ca0.9ZrO3
Pnma
a 5.61377 Å
b 5.75465 Å
c 8.03228 Å
V 259.4851 Å3
Intensity (arb. units)
2θ (degree)

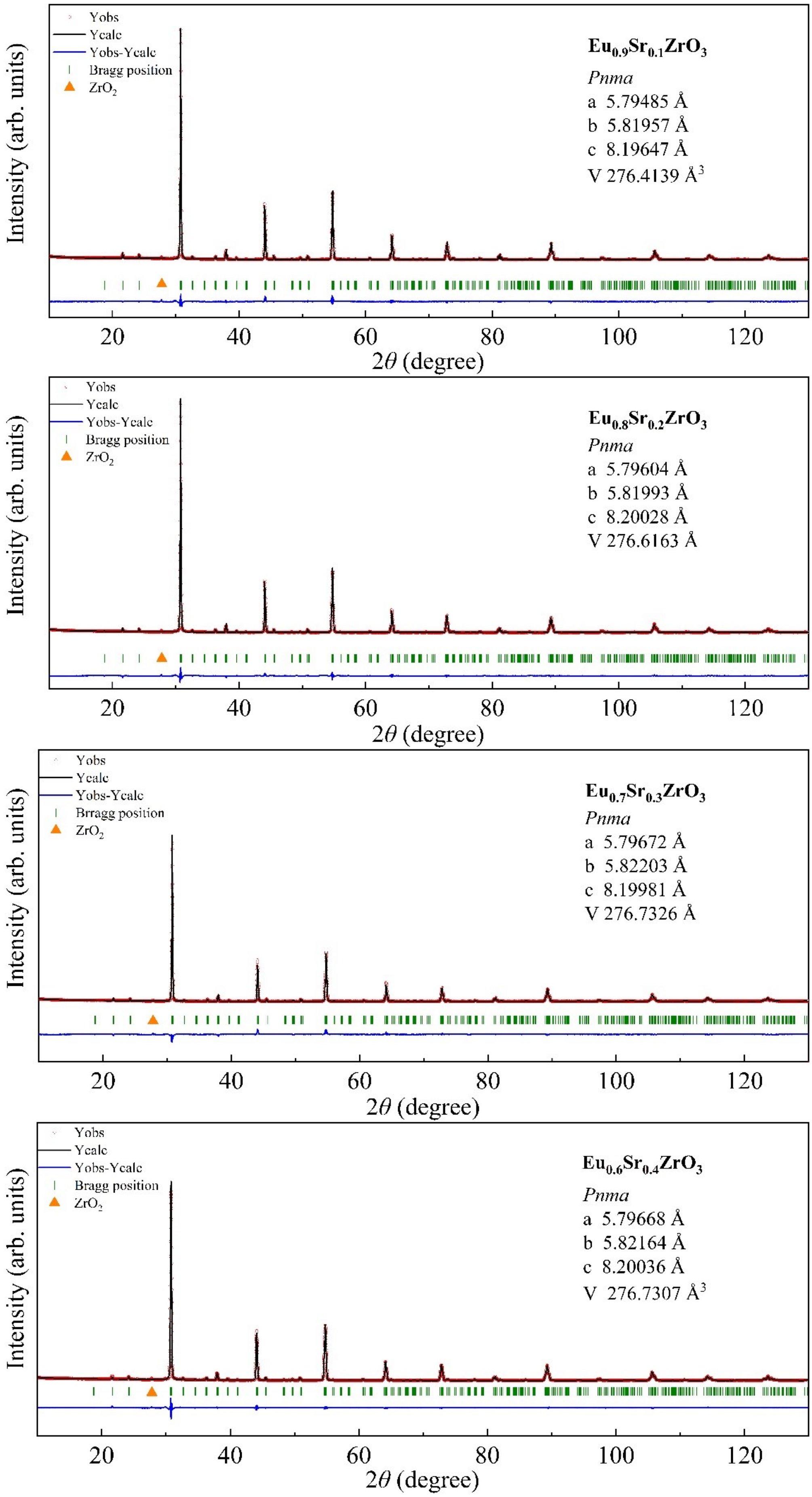

Yobs
Ycalc
Yobs-Ycalc
Bragg position
ZrO_2
$Eu_{0.9}Sr_{0.1}ZrO_3$
Pnma
a 5.79485 Å
b 5.81957 Å
c 8.19647 Å
V 276.4139 $Å^3$
Intensity (arb. units)
20 40 60 80 100 120
2*θ* (degree)
Yobs
Ycalc
Yobs-Ycalc
Bragg position
ZrO_2
$Eu_{0.8}Sr_{0.2}ZrO_3$
Pnma
a 5.79604 Å
b 5.81993 Å
c 8.20028 Å
V 276.6163 Å
Intensity (arb. units)
20 40 60 80 100 120
2*θ* (degree)
Yobs
Ycalc
Yobs-Ycalc
Brragg position
ZrO_2
$Eu_{0.7}Sr_{0.3}ZrO_3$
Pnma
a 5.79672 Å
b 5.82203 Å
c 8.19981 Å
V 276.7326 Å
Intensity (arb. units)
20 40 60 80 100 120
2*θ* (degree)
Yobs
Ycalc
Yobs-Ycalc
Bragg position
ZrO_2
$Eu_{0.6}Sr_{0.4}ZrO_3$
Pnma
a 5.79668 Å
b 5.82164 Å
c 8.20036 Å
V 276.7307 $Å^3$
Intensity (arb. units)
20 40 60 80 100 120
2*θ* (degree)

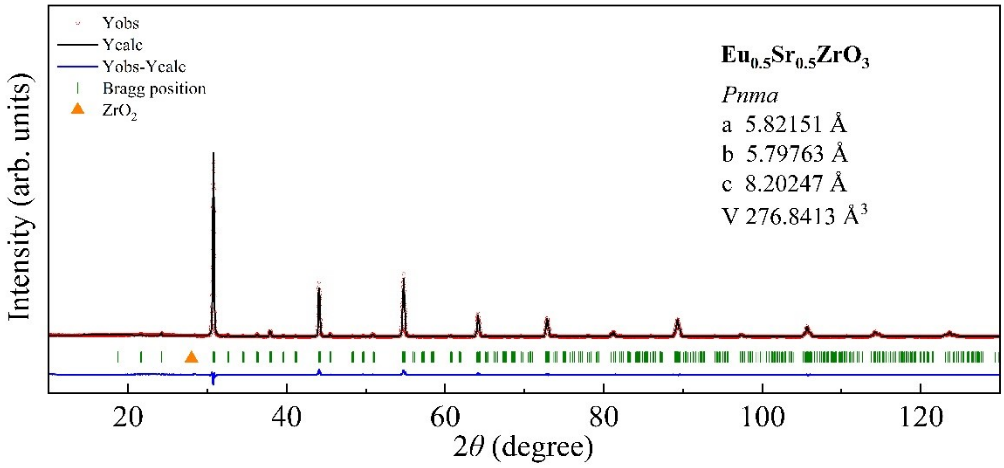

Fig. S1 X-ray diffraction profiles measured at room temperature (red crosses) and calculated profiles obtained by Rietveld analysis (black solid curves) for $A_xEu_{1-x}ZrO_3$ ($0 \leq x \leq 1$), where A is Ca, Sr, and Ba. The vertical ticks (green) indicate the positions of the Bragg reflections, and the bottom solid lines (blue) correspond to the difference between the observed and the calculated intensity. A small amount of ZrO_2 was detected as an impurity and marked with an orange triangle for $EuZrO_3$, $Ba_xEu_{1-x}ZrO_3$ ($0.4 \leq x \leq 0.9$), $Ca_xEu_{1-x}ZrO_3$ ($0.1 \leq x \leq 0.4$) and ($0.6 \leq x \leq 0.9$), and $Sr_xEu_{1-x}ZrO_3$ ($0.1 \leq x \leq 0.5$).

^{151}Eu Mössbauer spectrum

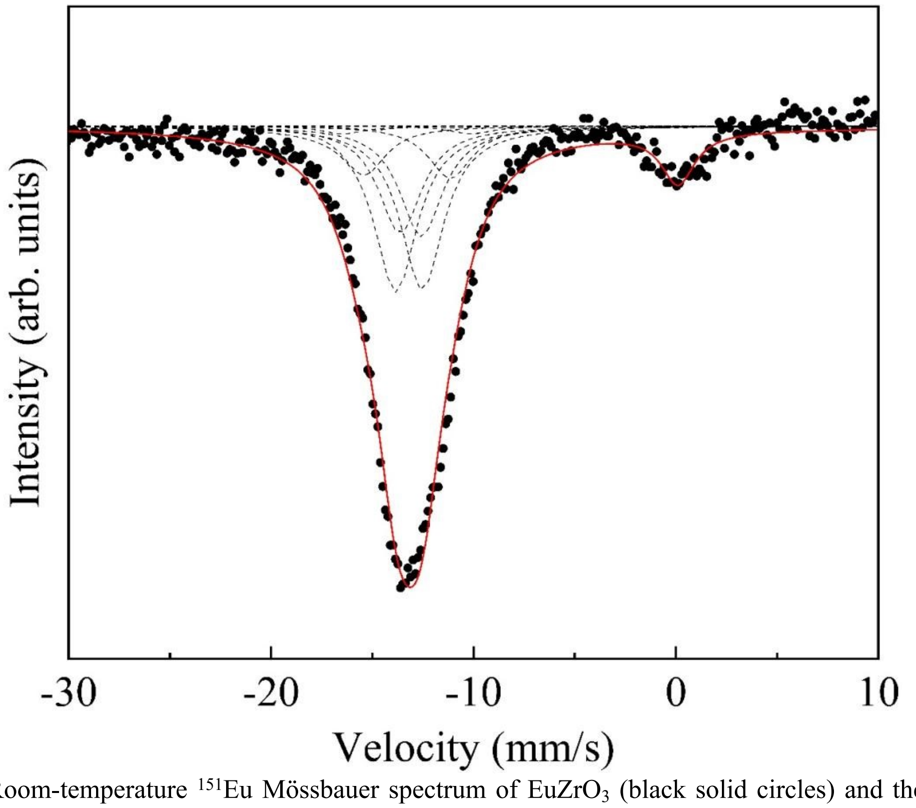

Fig. S2 Room-temperature ^{151}Eu Mössbauer spectrum of $EuZrO_3$ (black solid circles) and theoretical spectrum calculated by taking quadrupole interaction into account (red solid curve). The component lines of the 12 transitions are also shown for the Eu^{2+} absorption peak at around 12 mm/s. The Eu^{3+} absorption peak at around 0.5 mm/s was analyzed by a single Lorenzian.

Fig. S2 depicts room temperature ^{151}Eu Mössbauer spectrum of the $EuZrO_3$ sample. The spectrum exhibits a strong absorption peak assigned to Eu^{2+} at -12 ~ -14 mm/s and a weak absorption peak ascribed to Eu^{3+} at 0 ~ 1 mm/s. The Eu^{2+} absorption peak was fitted using the method described by Shenoy et al since this peak has been analyzed as a pure quadrupole spectral peak [60]. The Eu^{3+} absorption peak was fitted by a single Lorentzian. The fraction of absorption area of Eu^{2+} in the total absorption area due to europium ion ($A_{Eu^{2+}}/A_{Eu}$), the value of which is 0.94 as shown in Table S1, demonstrates that most of the europium ions are present as divalent state, confirming the efficiency of using ZrN as the reducing agent for the conversion of trivalent europium ions into divalent ones.

Table S1. The fitting parameters for ^{151}Eu Mössbauer spectrum of $EuZrO_3$.

$EuZrO_3$	$A_{Eu^{2+}}/A_{Eu}$	δ (mm/s)	γ (mm/s)	eQ_gV_{zz} (mm/s)	η (mm/s)
	0.94	-12.96(2)	2.41(6)	-10.20(37)	0.45(6)

$A_{Eu^{2+}}/A_{Eu}$: Fraction of absorption area of Eu^{2+} in total absorption area due to ^{151}Eu, δ: isomer shift relative to EuF_3 as a reference, γ: full width at half maximum of the Lorentzian, eQ_gV_{zz}: electric quadrupole interaction parameter, and $\eta = (V_{xx} - V_{yy})/V_{zz}$ asymmetry parameter, where e is the elementary charge, $V_{\sigma\sigma}$ is the electric field gradient in the σ direction and Q_g is the quadrupole moment of the nucleus in the ground state.

High-resolution X-ray fluorescence (HRXRF) spectrometry

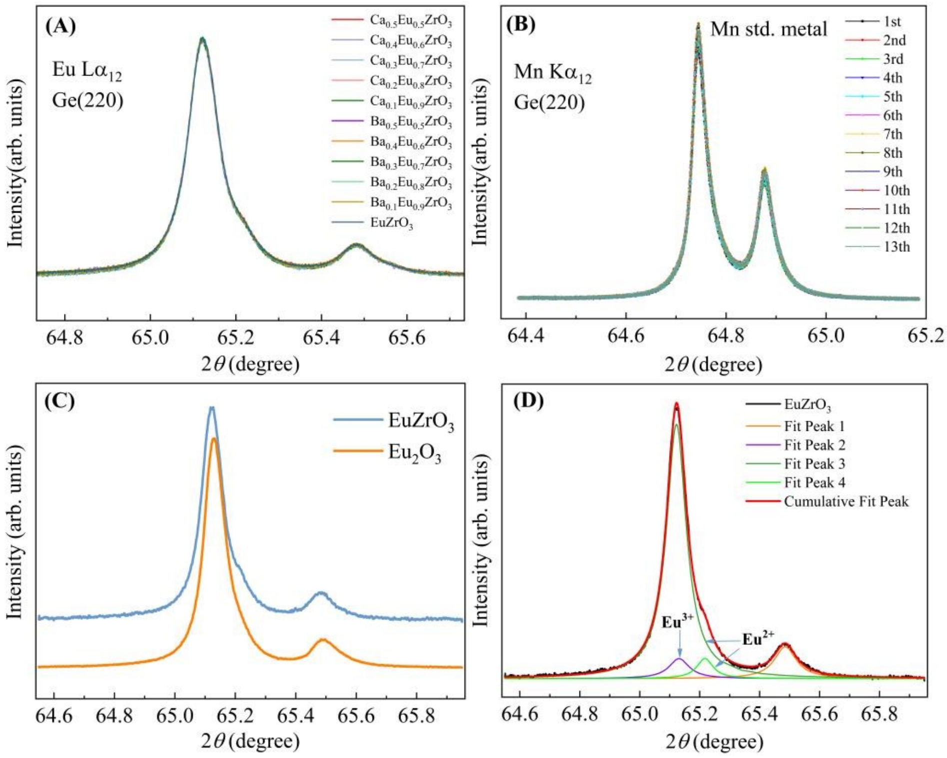

Fig. S3 High-resolution X-ray fluorescence (HRXRF) spectrometry. (a) Measured Eu $L_{\alpha12}$ spectra of $A_xEu_{1-x}ZrO_3$ ($0 \leq x \leq 0.5$), where A is Ca and Ba. The spectra are plotted after smoothing. All the spectra are completely overlapped with each other. (b) Measured Mn $K_{\alpha12}$ spectra of Mn metal as the standard before and after testing Eu $L_{\alpha12}$ spectra of $A_xEu_{1-x}ZrO_3$ and Eu_2O_3. (c) Measured Eu $L_{\alpha12}$ spectra of $EuZrO_3$ and Eu_2O_3. (d) Measured Eu $L_{\alpha12}$ spectra of $EuZrO_3$ (black curve) and fitted spectra (red curve) by Lorentzians. The Lorentzian peaks are displayed by different colors.

As shown in Fig. S3a, the spectra for all $A_xEu_{1-x}ZrO_3$ samples have almost the same peak positions and intensities and are completely overlapped with each other. The Mn $K_{\alpha12}$ standard spectra were shown in Fig. S3b for each sample. Compared to the Eu $L_{\alpha12}$ spectral peak of $EuZrO_3$ at 65.12°, the peak position for Eu_2O_3 at 65.13° is slightly different (Fig. S3c). Additionally, the Eu $L_{\alpha12}$ spectrum of $EuZrO_3$ displays a distinct shoulder at around 65.2°. Since the presence of trivalent Eu ions in $EuZrO_3$ is confirmed by ^{151}Eu Mössbauer spectrum, the main peak on the left is divided into three sub-peaks. The peak on the right in the Eu $L_{\alpha12}$ spectra of Eu_2O_3 and $EuZrO_3$ is found to have the same position at around 65.5°. To analyze the valence states of Eu in $EuZrO_3$, the Eu $L_{\alpha12}$ spectrum is deconvoluted into four Lorentzians (Fig. S3d). The parameters obtained by the fitting are listed in Table S2. The coefficient of determination

(R^2) value of 0.999 indicates the accuracy of the fitting method. Especially, the FWHM and peak position of peak 2 are consistent with the left main peak in the Eu $L_{\alpha 12}$ spectrum of Eu_2O_3 (trivalent Eu ions), revealing that the result is convincing. Since peak 3 and peak 4 attributed to divalent Eu ions form the left main peak combined with peak 2 in the Eu $L_{\alpha 12}$ spectrum of $EuZrO_3$, the value of peak 2 area divided by the total area of three peaks represents the molar ratio of trivalent Eu ions. The value is consistent with that obtained from the ^{151}Eu Mössbauer spectrum (6%). The presence of approximately 6% trivalent Eu ions in all $A_xEu_{1-x}ZrO_3$ samples is confirmed by HRXRF spectra with high consistency.

Table S2. The peak position (2θ), peak area (A), and full width at half maximum (FWHM) of Lorentzian peaks used for the analysis of the measured spectrum of $EuZrO_3$.

$EuZrO_3$	2θ (degree)	A	FWHM
Peak 1	65.4856	5.4258	0.0891
Peak 2	65.1311	2.9863	0.0819
Peak 3	65.1224	41.6294	0.0808
Peak 4	65.2176	2.7176	0.0659

Magnetic properties

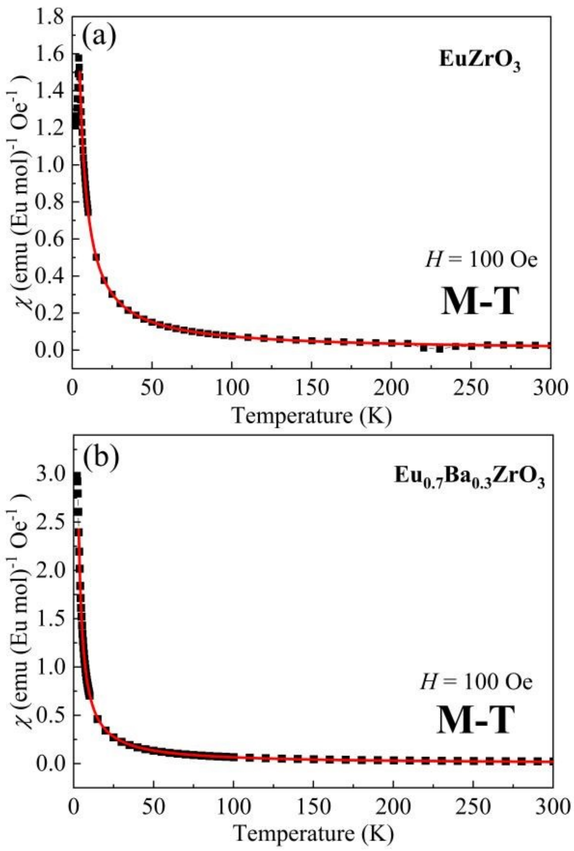

Fig. S4 Temperature dependence of magnetic susceptibility χ (T) for (a) $EuZrO_3$ and (b) $Ba_{0.3}Eu_{0.7}ZrO_3$ solid solution. Black squares represent the measured data. Red curves denote theoretical curves.

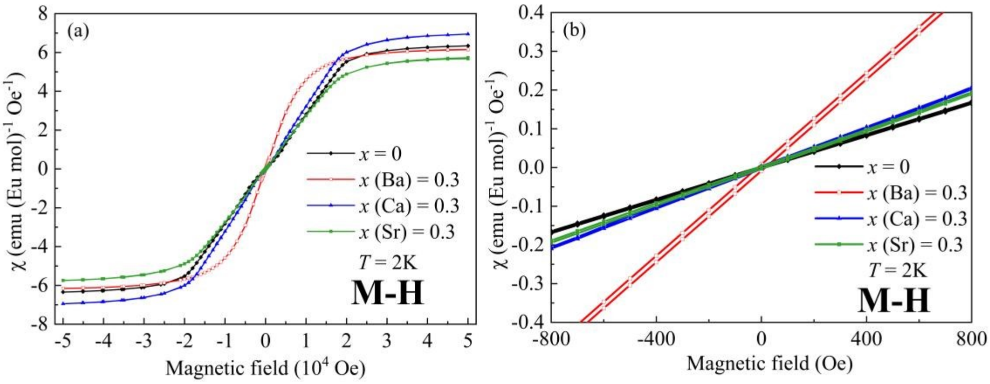

Fig. S5 Dependence of magnetic susceptibility on magnetic field at 2 K for (a) $EuZrO_3$ and $A_{0.3}Eu_{0.7}ZrO_3$ with A = Ba, Ca, and Sr. (b) Magnified view of (a).